

Venting of Runaway Reactions with Gas Generation

Joseph C. Leung

Fauske & Associates, Inc., Burr Ridge, IL 60521

Pressure relief venting of a runaway reaction with gas generation is examined in terms of the overall system response and the associated venting requirement. This article presents an exact formulation as well as an approximate analytical approach. The latter is shown to be particularly useful in vent-sizing applications. Using an aqueous hydrogen peroxide decomposition example, the analytical results are demonstrated to agree well with the exact numerical results over a wide range of overpressure. In addition, the analytical result is shown to reduce to the correct limit for a pure vapor system and offers a useful vent-sizing equation for a pure-gassy system.

Introduction

Emergency venting of reactors due to process upsets is a common industrial practice in pressure relief or reduction and is regarded as playing a vital role in the overall process safety and design. The research effort of the Design Institute for Emergency Relief Systems (DIERS) under the auspices of AIChE in the early 1980s has led to increased understanding of the venting technology (Fisher, 1985), with major emphasis on and application to the runaway reaction category. These are exothermic reactions that accelerate in rates exponentially with increasing temperatures. From the standpoint of pressure relief and vent sizing, three major classes of runaway reactions have been described: the "vapor" system, the "gassy" system, and the "hybrid" system (Leung and Fauske, 1987). The vapor or boiling system refers to those that exert their own vapor pressure on the process vessel. Inherent in this system is the capability for latent heat of cooling via boiling, which is counted on to cause a temperature turnaround during venting. The gassy system, on the other hand, has no evaporative cooling potential since the gases produced are above their critical points. Thus, temperature turnaround prior to complete reaction cannot be achieved simply by venting. Finally, the hybrid system can fall anywhere between these two limiting cases: the pure vapor case and the pure gassy case. Up to now, most of the publications on venting technology have dealt with the vapor system only (Duxbury, 1980; Huff, 1982; Fauske, 1984; Leung, 1986, 1987). Increasingly, the gassy system and the hybrid system are recognized to have industrial importance, but the vent sizing methodology has not been as well developed and

validated as the vapor system (Huff, 1984; Leung and Fauske, 1987).

The purpose of this article is to present a coherent treatment for the general case of venting a hybrid runaway reaction system for a batch reactor. Attention is focused on the analytical solutions, for which useful results for vent sizing application will be extracted. This analytical treatment has an advantage in revealing important parameters or dimensionless groups for runaway reaction characterization. Furthermore, such a general treatment will be shown to yield limiting solutions for the vapor system and the gassy system.

We will begin the discussion with the governing equations for describing the pressure relief venting of a hybrid system; this will be followed by the analytical approach and its solution procedure. Finally, an example will be presented to illustrate its vent sizing application.

Governing Equations

Governing equations for venting of a hybrid system are obtained from the macroscopic balance on the vessel as shown in Figure 1. These unsteady conservation equations are:

$$\frac{dm}{dt} = -W \quad (1)$$

$$\frac{dm_g}{dt} = m \dot{m}_g - W x_{gi} \quad (2)$$

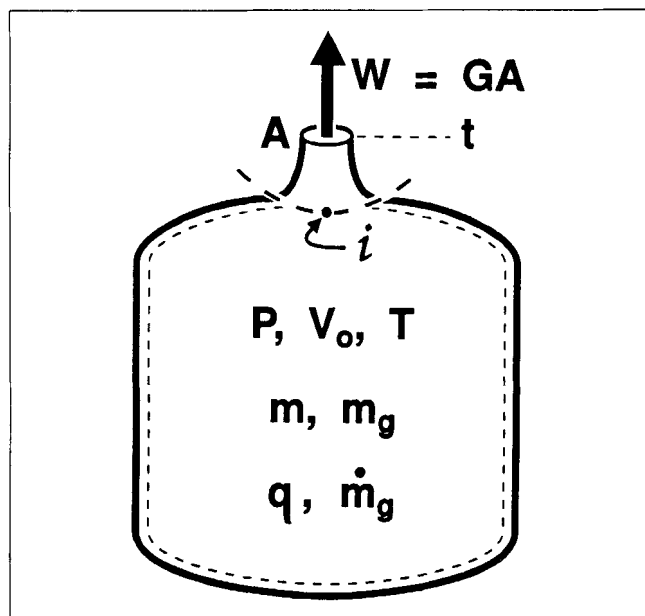


Figure 1. Reference reactor for model development.

$$\frac{dT}{dt} = \left[m q - W v_i \frac{h_{vf}}{v_{vf}} \right] / (m C_p) \quad (3)$$

where Eqs. 1 through 3 represent total mass balance, gas component mass balance, and a special form of the energy balance (Leung, 1986), respectively. In these equations, W is known as the relief vent rate that is equal to the discharge mass flux G multiplied by the appropriate vent area A , \dot{m}_g is the specific gas generation rate (kg gas/kg·s), q is the specific energy release rate, x_{gi} is the gas mass fraction in the vented stream, and v_i is the specific volume of the vented stream. In addition, equations of state are necessary to provide partial pressure relationship. The equation of state for the vapor or boiling component can be represented adequately by a two-constant Antoine-type expression:

$$P_v = \exp \left(a - \frac{b}{T} \right) = \exp \left[a - \frac{h_{vf} M_{wv}}{RT} \right] \quad (4)$$

where $b = (h_{vf} T) / (v_{vf} P_v) \approx h_{vf} M_{wv} / R$ via the Clausius-Clapeyron relation. As for the gas component, ideal gas law is assumed:

$$P_g = \frac{m_g RT}{M_{wg} V_g} = \frac{m_g RT}{M_{wg} (V_o - m v_i)} \quad (5)$$

Finally, the total pressure of the system is given by the sum of the partial pressures:

$$P = P_v + P_g \quad (6)$$

In the present development we shall treat the particular case of no disengagement of vapor/gas from the liquid within the vessel, the so-called uniform-froth or homogeneous-vessel

venting regime. In this case, the vessel exit quality and specific volume assume the bulk average values: $x_{gi} = x_g = m_g / m$ and $v_i = v = V_o / m$.

Discharge Flow Evaluation

To provide closure of the problem, we have to couple the discharge flow evaluation with the solution of the above set of differential equations. Here the discharge flow is commonly treated in a quasisteady-state manner (Bird et al., 1960), and for simplicity only the case of a frictionless nozzle is considered here. The hybrid case of flashing (boiling two-phase) flow in the presence of noncondensable gases can be most conveniently evaluated by the recent method of Leung and Epstein (1991). The resulting nozzle flow of such a hybrid mixture under homogeneous equilibrium assumption can be described by the general mass flux equation:

$$G^* = \left\{ 2 \left[-\alpha y_g \ln \frac{P_{gt}}{P_g} + (1-\alpha) y_g \left(1 - \frac{P_{gt}}{P_g} \right) - \omega (1-y_g) \ln \frac{P_{vt}}{P_v} + (1-\omega)(1-y_g) \left(1 - \frac{P_{vt}}{P_v} \right) \right] \right\}^{1/2} \left[\omega \left(\frac{P_v}{P_{vt}} - 1 \right) + 1 \right] \quad (7)$$

where $G^* = G / \sqrt{P/v} = G / \sqrt{P\rho}$, a normalized mass flux (mass flow per unit area). Note that the subscript t denotes the nozzle throat condition, and all other variables are evaluated at the inlet to the vent (here subscript i has been dropped for convenience). The ω parameter in Eq. 7 is defined in terms of the following stagnation properties:

$$\omega = \frac{x v_v + \frac{C_p T P_v}{v} \left(\frac{v_{vt}}{h_{vf}} \right)^2}{v} \approx \alpha + (1-\alpha) \frac{C_p T P_v}{v_i} \left[\frac{v_{vt}}{h_{vf}} \right]^2 = \alpha + (1-\alpha) \omega_s \quad (8)$$

During the expansion process through the converging nozzle, these partial pressures are related via (Leung and Epstein, 1991):

$$\alpha \left(\frac{P_g}{P_{gt}} - 1 \right) = \omega \left(\frac{P_v}{P_{vt}} - 1 \right) \quad (9)$$

Equation 7 shows that as the downstream pressure is reduced, the normalized two-phase mass flux G^* reaches a maximum corresponding to a so-called choking condition. This maximum can be found by setting the derivative dG/dP to zero, yielding:

$$\begin{aligned} & -\alpha y_g \ln \frac{P_{gt}}{P_g} + (1-\alpha) y_g \left(1 - \frac{P_{gt}}{P_g} \right) \\ & - \omega (1-y_g) \ln \frac{P_{vt}}{P_v} + (1-\omega)(1-y_g) \left(1 - \frac{P_{vt}}{P_v} \right) \\ & = \frac{1}{2} \left[\frac{y_g}{\alpha} \left(\frac{P_{gt}}{P_g} \right)^2 + \frac{(1-y_g)}{\omega} \left(\frac{P_{vt}}{P_v} \right)^2 \right] \left[\omega \left(\frac{P_v}{P_{vt}} - 1 \right) + 1 \right]^2 \end{aligned} \quad (10)$$

This is a transcendental equation for either P_{gt}/P_g or P_{vt}/P_v

as they are to be solved simultaneously with Eq. 9 for these "critical" pressure ratios. Once these ratios are found, the overall critical (choking) pressure ratio is given by:

$$\frac{P_c}{P} = y_g \frac{P_{gt}}{P_g} + (1 - y_g) \frac{P_{vt}}{P_v} \quad (11)$$

In the case where the ambient pressure P_a is higher than the choking exit pressure P_c , an unchoked or subsonic flow condition, Eq. 9 is solved for P_{gt}/P_g and P_{vt}/P_v subject to the obvious constraint that P_{gt} and P_{vt} add up to P_a . Substitution of these pressure ratios into Eq. 7 will yield the unchoked mass flux. This unified scheme has been demonstrated (Leung and Epstein, 1991) to yield meaningful solutions spanning the entire range of hybrid two-phase flow, from pure flashing flow at one end ($y_g = 0$) to pure nonflashing flow at the other ($y_g = 1$).

Analytical Solution

Here we seek an analytical solution for the purpose of providing useful results in vent sizing application. In so doing, key scaling parameters can be revealed. Equations 1 through 3 can be easily integrated analytically if one makes the following simplifying assumptions:

1. Constant vent rate W
2. Constant q and \dot{m}_g
3. Constant physical properties.

These assumptions, similar to those employed in an earlier development with the vapor system (Leung, 1986), do not result in unacceptable solutions when compared to the exact calculations, as will be demonstrated.

To facilitate integration and presentation of the results, the following dimensionless variables are defined:

$$\begin{aligned} m^* &\equiv m/m_o \\ m_g^* &\equiv \frac{m_g}{m_o} \frac{v_{go}}{v_o} \frac{W_{vo}}{W_{go}} = \frac{m_g}{m_o m_g (m_o/W_{vo})} \\ T^* &\equiv T/T_o \\ P_v^* &\equiv P_v/P_{vo} \\ P_g^* &\equiv P_g/P_{go} \\ P^* &\equiv P/P_o \\ t^* &\equiv t/t_e \end{aligned} \quad (12)$$

where

$$t_e \equiv \frac{m_o}{W} \quad (13)$$

$$W_{vo} \equiv \frac{m_o q}{h_{vbo}} \frac{v_{vbo}}{v_o} \quad (14)$$

$$W_{go} \equiv m_o \dot{m}_g \frac{v_{go}}{v_o} \quad (15)$$

Here the subscript o refers to the initial value at time zero,

and with the exception of m_g^* and t^* , the above dimensionless variables are defined relative to their initial values. Here W_{vo} and W_{go} are termed the fundamental vent rates for vapor generation and gas generation, respectively, and have units of kg/s; their significance will be discussed later.

Equations 1 through 3 can be integrated with the above assumptions to yield, respectively:

$$m^* = 1 - t^* \quad (16)$$

$$m_g^* = \left[m_{go}^* + \frac{t^*}{W/W_{vo}} \right] (1 - t^*) \quad (17)$$

$$\Delta T^* = T^* - 1 = \frac{(T_o/b)}{(1 - \alpha_o)\omega_s} \left[\frac{t^*}{W/W_{vo}} - \frac{t^*}{1 - t^*} \right] \quad (18)$$

while Eqs. 4 through 6 can also be rewritten in terms of dimensionless variables as:

$$P_v^* = \exp \left[\frac{b}{T_o} \left(1 - \frac{1}{T^*} \right) \right] \quad (19)$$

$$P_g^* = \frac{\left[1 + \frac{t^*}{\alpha_o W/W_{go}} \right] (1 - t^*) T^*}{1 + \left(\frac{1 - \alpha_o}{\alpha_o} \right) t^*} \quad (20)$$

$$P^* = (1 - y_{go}) P_v^* + y_{go} P_g^* \quad (21)$$

Hence, for a given relief vent rate W , Eqs. 16 through 21 provide time-dependent representations of mass, temperature and pressure, which were shown in Figure 2 for two widely different hybrid systems. In a nearly gassy system, Figure 2a, both temperature and pressure exhibit their maximum at different times, a direct result of the presence of the gas and its accumulation behavior in the vessel. In a nearly vapor system, Figure 2b, on the other hand, both temperature and pressure turn around almost cocurrently.

For vent sizing, we are most concerned with the maximum pressure attained during a venting scenario, especially with the amount of overpressure (that is, pressure increase above the relief set pressure). This overpressure can be evaluated readily from the above set of equations if one can determine the time at which peak pressure occurs, the so-called turnaround time. Mathematically this is determined by setting dP/dt or dP^*/dt^* to zero, and solving for t . To keep the mathematic tractable, some approximations are necessary in the evaluation of the derivative dP_g/dt . First, the thermal effect is ignored in that T^* in Eq. 20 is assumed to be constant at close to unity. In addition, we also assume $x_{go} \ll x_g$, that is, the initial gas mass fraction at the start of venting is smaller than that accumulated at the turnaround time. Thus, from Eq. 20 we obtain the derivative:

$$\frac{dP_g^*}{dt^*} = \frac{1}{(1 - \alpha_o)} \frac{T^*}{W/W_{go}} \frac{\left[\frac{\alpha_o}{1 - \alpha_o} (1 - 2t^*) - t^{*2} \right]}{\left(\frac{\alpha_o}{1 - \alpha_o} + t^* \right)^2} \quad (22)$$

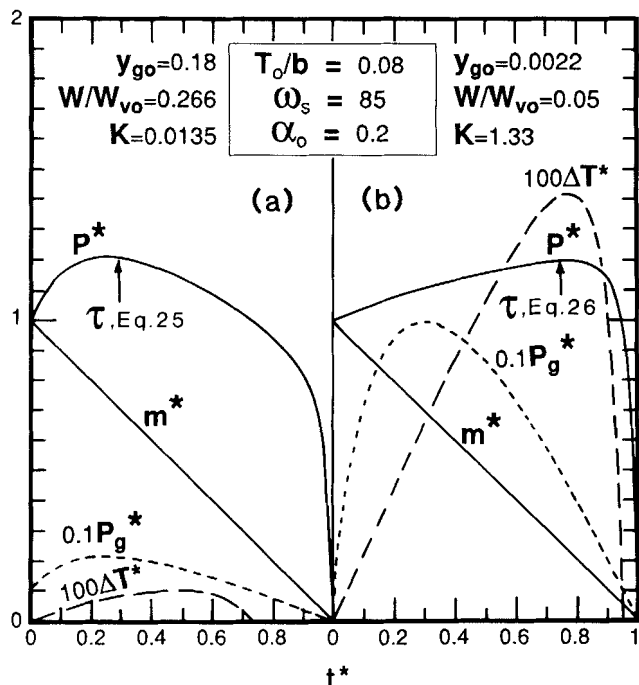


Figure 2. Analytical results of venting behavior for two hybrid systems: (a) a nearly gassy system and (b) a nearly vapor system.

The vapor-pressure time derivative dP_v^*/dt^* is obtained from Eq. 19, where dT^*/dt^* is evaluated from Eq. 18. Upon substitution into the differential form of Eq. 21 and setting dP^*/dt^* to zero, a transcendental equation for the dimensionless turnaround time τ is finally obtained:

$$\frac{y_{go}}{\alpha_o} W_{go} \left[\frac{\frac{\alpha_o}{1-\alpha_o} (1-2\tau) - \tau^2}{\frac{1-\alpha_o}{\alpha_o} \left(\tau + \frac{\alpha_o}{1-\alpha_o} \right)^2} \right] + \frac{(1-y_{go})}{(1-\alpha_o)\omega_s} W_{vo} \left[1 - \frac{W/W_{vo}}{(1-\tau)^2} \right] = 0 \quad (23)$$

According to this result, the turnaround time depends on the initial void fraction α_o , the normalized vent rate W/W_{vo} , and the following dimensionless group, here termed the "hybrid system parameter,"

$$K = \frac{(1-y_{go})}{y_{go}} \frac{\alpha_o}{(1-\alpha_o)\omega_s} \frac{W_{vo}}{W_{go}} \quad (24)$$

This K parameter is a useful delineator between the vapor system and the gassy system. A small K value characterizes a gassy system such that τ can be given by:

$$\tau = \frac{\alpha_o^{0.5}}{1 + \alpha_o^{0.5}} \quad (25)$$

This can be obtained from Eq. 23 with $W_{vo}=0$ or from Eq.

22 by letting $dP_g^*/dt^*=0$. Interestingly enough, this result is independent of the relief vent rate W and τ depends only on α_o , the initial void fraction in the reactor. On the other end, a large K value reflects a vapor system such that:

$$\tau = 1 - \left(\frac{W}{W_{vo}} \right)^{1/2} \quad (26a)$$

This result, as obtained from Eq. 23 with $W_{go}=0$, will be shown to be in perfect agreement with an earlier publication on pure vapor system (Leung, 1986). Figure 3 shows a solution for $\alpha_o=0.2$ with the variation of the dimensionless turnaround time with K and the asymptotic behavior at both small and large K values. These asymptotic turnaround times are shown to correlate well with the pressure turnaround points for the two extreme hybrid systems in Figure 2. The hybrid system parameter K therefore provides a measure of the relative proximity to each limiting system and is a useful indicator for characterizing the particular runaway reaction system.

Vent Sizing Applications

A major objective of this work was to formulate a vent sizing methodology for hybrid systems. The above-mentioned analytical approach will be evaluated and compared against the exact numerical calculation using the following runaway reaction example. A storage tank for aqueous hydrogen peroxide solution is inadvertently contaminated with iron (a catalyst for decomposition), and the peroxide begins to decompose, generating both gas (oxygen) and heat. Since the tank is well insulated, the reaction heat is retained as sensible heat, giving rise to faster decomposition in accordance with the Arrhenius law. This 1.136-m³ tank has a design pressure of 3.45 bar·g and is to be protected with a relief device set to open at 0.345 bar·g. For design purposes, we shall ignore the vessel wall heat capacity and assume homogeneous-vessel (uniform-froth) venting. The pertinent parameters are in Table 1. Specific Reaction Rate Data (per unit mass of solution basis):

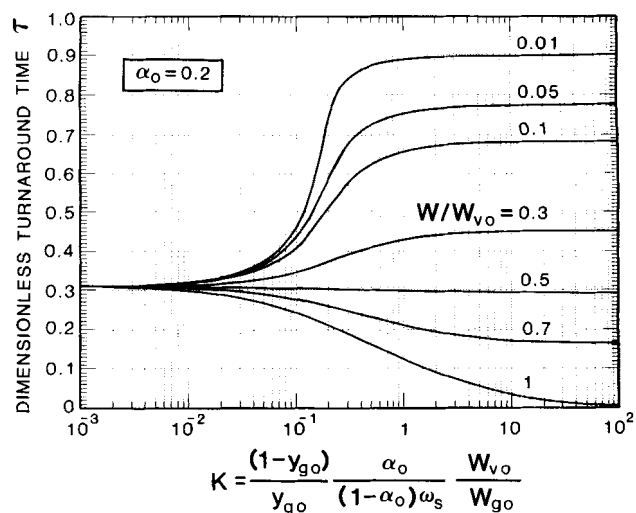


Figure 3. Generalized presentation of dimensionless turnaround time.

Table 1. Parameters for H₂O₂ Venting Example

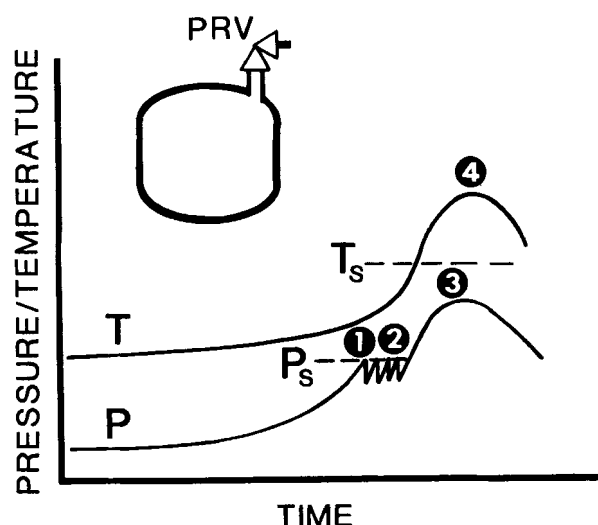
Stoichiometry	$\text{H}_2\text{O}_{2(l)} \rightarrow \text{H}_2\text{O}_{(l)} + \frac{1}{2} \text{O}_{2(g)}$
Tank Volume	$V_o = 1.136 \text{ m}^3$
Solution Mass	$m_o = 907 \text{ kg}$
Initial Concentration	25% wt. (15% mol) H ₂ O ₂
Fill Ratio	$1 - \alpha_o = 0.8$
Vapor Molecular Weight	$M_{wv} = 18$ (mostly steam)
Gas Molecular Weight	$M_{wg} = 32$ (oxygen)
Runaway Onset Temperature	$T_{on} = 50^\circ\text{C}$
Liquid Specific Heat	$C_p = 4 \text{ kJ/kg}\cdot\text{K}$
Liquid Specific Volume	$v_l = 0.001 \text{ m}^3/\text{kg}$
Vapor Pressure	$P_v = \exp\left(24.27 - \frac{4,795}{T(\text{K})}\right) \text{ N/m}^2$
Vapor-Specific Volume	$v_v = RT/P_v/M_{wv}$
Gas-Specific Volume	$v_g = RT/P_g/M_{wg}$
Latent Heat of Vaporization	$h_{vl} = bR/M_{wv} = 2,215 \text{ kJ/kg}$

$$q(\text{J/kg}\cdot\text{s}) = 933 \exp\left[\frac{23,000}{1.987}\left(\frac{1}{373.16} - \frac{1}{T}\right)\right]$$

$$\dot{m}_g(\text{kg O}_2/\text{kg}\cdot\text{s}) = 1.6 \times 10^{-4} \exp\left[\frac{23,000}{1.987}\left(\frac{1}{373.16} - \frac{1}{T}\right)\right]$$

The above reaction rate data were obtained experimentally using an adiabatic calorimeter for runaway reaction (Leung et al., 1986). The heat release rate was calculated from temperature rise data which gave a rate of $14^\circ\text{C}/\text{min}$ at 100°C . The specific gas generation rate \dot{m}_g was determined by the pressure rise data. As implied by the above rate expression, a zeroth-order reaction model is assumed, and this is considered adequate in the region of interest for the present study.

The initial condition corresponding to the start of two-phase venting from the vessel may vary. Figure 4 shows a typical venting scenario for a hybrid system. Here the pressure relief valve (PRV) will "lift" first and bleed off the accumulated


Figure 4. Venting scenario for a hybrid reaction system.

gas when the system pressure attains the relief set pressure (Pt. 1 of Figure 4). The lifting and reclosing of the PRV may occur many times, while the vapor pressure of the volatile component continues to increase due to rising temperature. It is not anticipated, however, that significant two-phase discharge would occur during these early periodic relief intervals. In fact, it would not be conservative to assume two-phase release in these periods, because such a release involving liquid content has the merit of getting rid of the reactant early when the reaction rates are comparatively low. However, as the boiling point of the vapor component is approached, the vapor pressure contribution noticeably increases, and the total vapor and gas volumetric rate rises rapidly. For a conservative design, this is the point where the two-phase discharge, simultaneous with overpressure venting, will take place (Pt. 2 of Figure 4). Of course, this is an idealized situation where the transition to two-phase venting occurs quite abruptly, but this conservative assumption is currently most amenable for analysis. For an adequately sized relief vent, pressure will turn around before the vessel design pressure is reached. Due to the effect of gas accumulation, pressure and temperature turnarounds do not occur at the same time (Pts. 3 and 4 of Figure 4).

The so-called tempering condition is achieved when the evaporative heat removal becomes equal to the reaction heat release (Huff, 1982). At this condition, the reaction is said to be "tempered" and the temperature rise is halted. This condition has been determined experimentally for the present reaction at the given set pressure of $0.345 \text{ bar}\cdot\text{g}$. For our analysis, the partial pressures are proportional to the molar generation rate at the tempering point:

$$\frac{P_g}{P_v} = \frac{x_g/M_{wg}}{x_v/M_{wv}} = \left(\frac{\dot{m}_g}{M_{wg}}\right) / \left(\frac{q}{h_{vl}M_{wv}}\right) \quad (27)$$

In addition, these partial pressures add up to the system total pressure. For vent sizing purposes, one is most interested in determining the tempering temperature T_{TP} at the relief device set pressure P_s . Thus, with P equal to P_s , we can solve for T_{TP} , which yields the following vapor pressure:

$$P_v(T_{TP}) = \frac{P_s}{1 + \frac{P_g}{P_v}} \quad (28)$$

At $0.345 \text{ bar}\cdot\text{g}$, this equation together with Eq. 27 yields a tempering temperature of 106°C for the peroxide solution, which is in excellent agreement with the experimental determination. This tempering temperature will be taken to be the "set temperature" coinciding with the onset of two-phase venting. It should be noted, however, that the above analytical approach can be used to describe the homogeneous-vessel venting behavior prior to attaining such a tempering temperature, but the result may not be conservative for vent sizing design for the reason given above.

Evaluating the properties at the tempering point (106°C , $0.345 \text{ bar}\cdot\text{g}$) corresponding to the set pressure, we obtain:

$$\alpha_o = 0.2$$

$$y_{go} = 0.18$$

$$\begin{aligned}
 \omega_s &= 85 \\
 q_s &= 1,530 \text{ J/kg}\cdot\text{s} \\
 \left(\frac{dT}{dt}\right)_{adi} &= 22.9^\circ\text{C/min} \\
 \dot{m}_g &= 2.61 \times 10^{-4} \text{ kg/kg}\cdot\text{s} \\
 v_{vo} &= 1.568 \text{ m}^3/\text{kg} \\
 v_{go} &= 4.076 \text{ m}^3/\text{kg} \\
 W_{vo} &= 780 \text{ kg/s} \\
 W_{go} &= 772 \text{ kg/s} \\
 T_o/b &= 0.079 \\
 K &= 0.0135
 \end{aligned}$$

Here, we find that the two fundamental vent rates (W_{vo} and W_{go}) are approximately equal, a direct result of the conditions implied by Eq. 27. Therefore, at the tempering point the hybrid system parameter K is governed by only three parameters y_{go} , α_o , and ω_s , as seen from Eq. 24.

The analytical results can be obtained as follows. For a chosen normalized relief vent rate W/W_{vo} , Eq. 23 is solved for τ . Substitution of τ into Eqs. 16 through 20 would yield m^* , m_g^* , T^* , P_v^* , P_g^* at the peak overpressure ΔP . From T^* at pressure turnaround, the corresponding temperature T_m and energy release rate q_m are evaluated. An average energy release rate during the overpressure period is evaluated based on a simple average $\bar{q} = (q_s + q_m)/2$, while the fundamental vent rate for vapor production W_{vo} , as defined by Eq. 14, is calculated based on this \bar{q} average value. Now with W_{vo} and W/W_{vo} known, the required vent rate W yielding the calculated ΔP can be found.

Figure 5 compares the required vent rates from the analytical method and the exact numerical calculations. The latter was

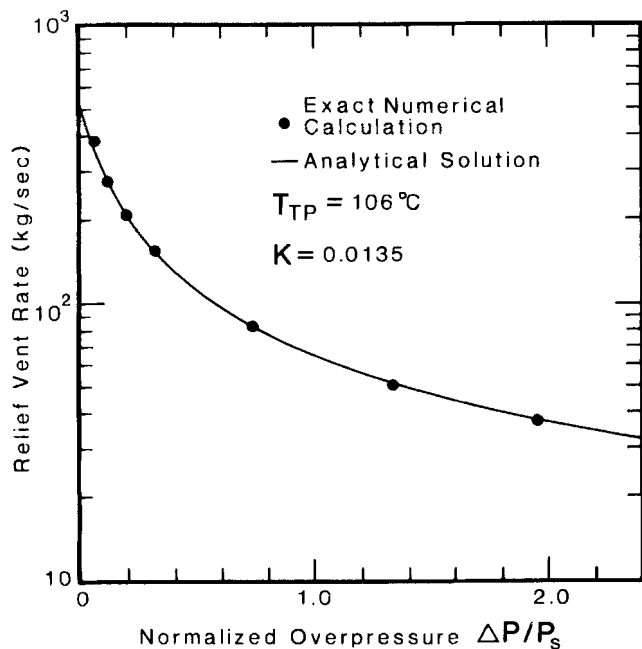


Figure 5. Relief vent rate vs. normalized overpressure.

performed using a selected vent area and a Euler integration scheme with a time step of $t_e/1,000$. In the numerical integration scheme, the physical properties and the discharge mass flux were updated in every time step. Note that the vent rate in the numerical case actually varies with time, but an average rate during the overpressure period can be defined by the net mass loss divided by the turnaround time. Figure 5 demonstrates that for a wide range of overpressure, the analytical solutions for these vent rates are in excellent agreement with the exact solutions. Figure 6 compares the transient venting behavior at two different vent rates: case 1 with $W=211$ kg/s and case 2 with $W=37.5$ kg/s. The assumption of a constant vent rate W in the analytical solution is clearly an oversimplification, since it overestimates W later in the venting process. As a result, the peak temperature and peak vapor pressure during venting are underestimated, but this occurs well after the system pressure turnaround.

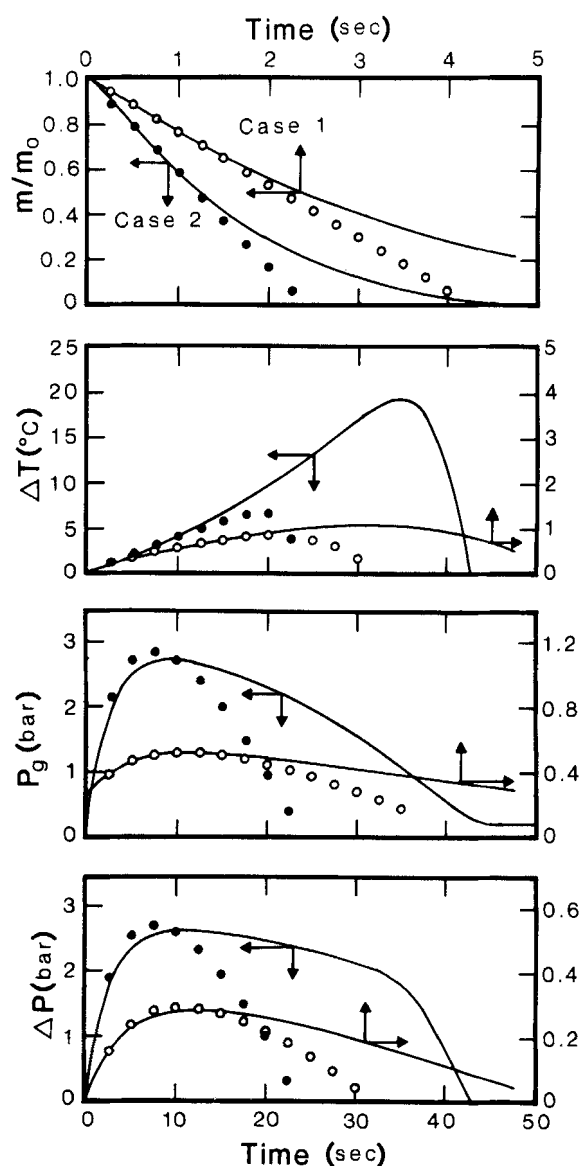


Figure 6. Venting behavior: analytical results (\bullet , \circ) vs. exact numerical solutions (—).

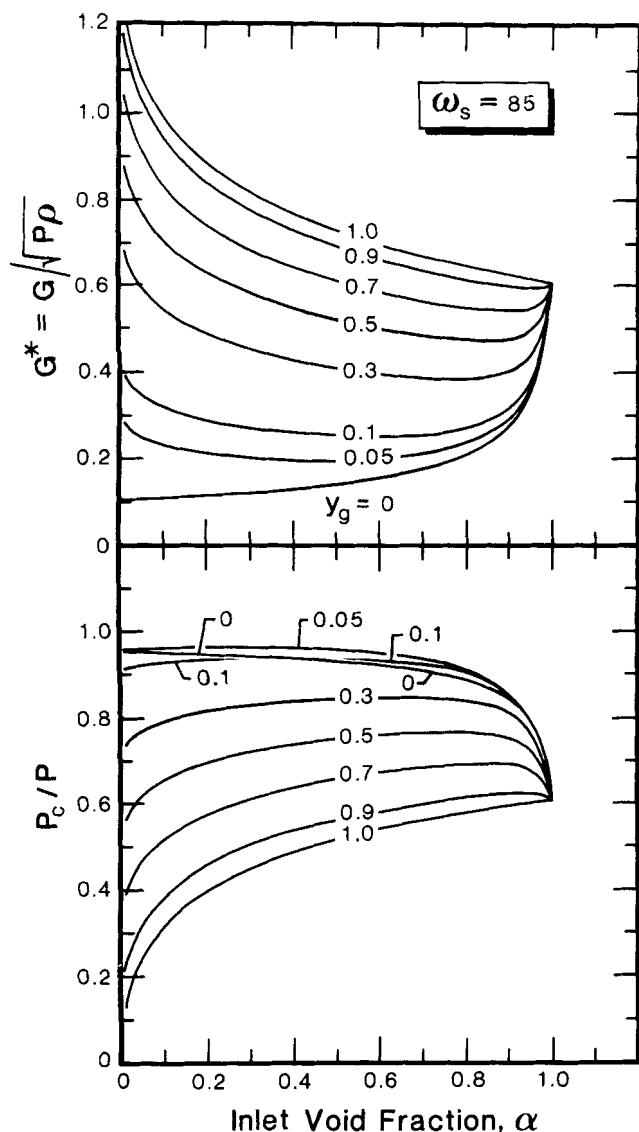


Figure 7. Generalized mass flux presentation for hybrid two-phase choked flow for $\omega_s = 85$.

As far as the amount of overpressure is concerned, the analytical solutions are in good agreement with the exact solution. The maximum overpressure occurs early in these venting processes, and in this particular hybrid system the behavior is essentially gassy in nature: the calculated overpressure is due entirely to gas accumulation (compare P_g with ΔP in Figure 6). Referring to Figure 3, at a K value of 0.0135, the dimensionless turnaround time is nearly independent of vent rate; this is characteristic of a gassy system. Here we find that $\tau = 1 - m/m_o = 0.3$ (from Figure 3), or simply $m/m_o = 0.7$ at the peak pressure. This observation is confirmed by the results obtained for these two widely differed vent rates in Figure 6. For vent sizing evaluations, the excellent agreement in required vent rate vs. overpressure, as demonstrated in Figures 5 and 6, clearly supports the approximations and the key assumptions employed in the analytical method.

To obtain the resulting vent area A from the calculated W in the analytical method, a representative mass flux G has to

be estimated. According to the theoretical model presented earlier, G^* is uniquely defined by α , ω , and y_g . For these three variables, average values during the overpressure period can be estimated from:

$$\bar{\alpha} = 1 - 0.5(1 - \alpha_o)(1 + m^*) \quad (29)$$

$$\bar{\omega} = \bar{\alpha} + (1 - \bar{\alpha})\omega_s \quad (30)$$

$$\bar{y}_g = 0.5y_{go} \left(1 + \frac{P_g^*}{P^*} \right) \quad (31)$$

It is noted here that ω_s as defined by Eq. 8 assumes a constant value throughout for simplicity (that is, it takes on the initial value at time zero). A generalized solution for G^* can be represented by Figure 7 for a ω_s value of 85 pertaining to this example. With G^* evaluated, the resulting mass flux can be calculated as follows:

$$G = G^* \sqrt{\frac{P_o m_o}{V_o}} \frac{\sqrt{(1 + P^*)(1 + m^*)}}{2} = \frac{G^*}{2} \sqrt{\frac{(P_o + P_m)(m_o + m_m)}{V_o}} \quad (32)$$

while the ideal vent area is simply:

$$A = W/G \quad (33)$$

Figure 8 compares these vent areas based on the analytical method against the vent areas used in the exact calculations. The agreement is seen to be satisfactory over a wide range of overpressure. More importantly the vent areas based on the analytical approach are somewhat larger (more conservative),

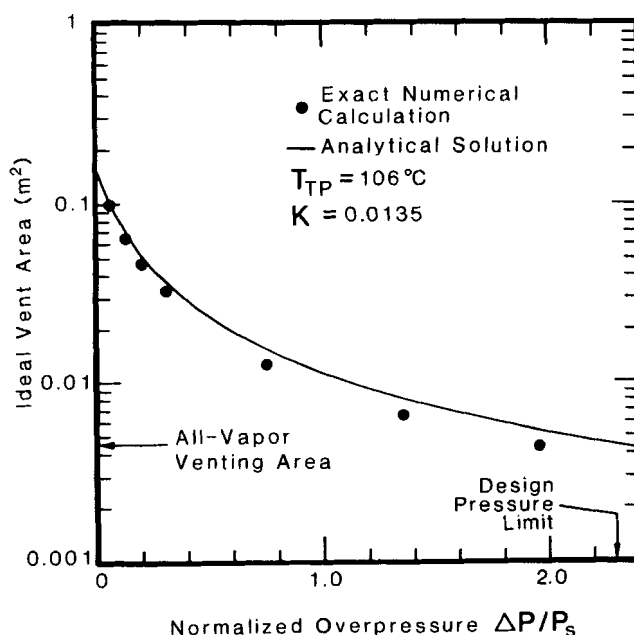


Figure 8. Vent area prediction vs. normalized overpressure.

ranging from 10% at $\Delta P/P_o = 0.2$ to 20% at $\Delta P/P_o = 2$. Because of this conservative design feature, there is little incentive to refine the simple averaging scheme employed in Eqs. 29 through 32 to come up with a better estimate of G , and hence A . Figure 8 also demonstrates the significant reduction in vent size by allowing for overpressure. This behavior is similar to that discovered for the vapor system (Leung, 1986). The ability to remove mass (chemical fuel) via two-phase venting gives rise to a much reduced total energy release rate and gas generation rate at the pressure turnaround condition if some overpressure is allowed. In this illustration, the area reduction at $\Delta P/P_o$ of 0.8 is quite significant, about tenfold smaller than the zero overpressure case.

It is also revealing to examine the venting requirement for vapor venting only. In this case, the required vent rate is equated to the sum of the vaporization rate and the gas generation rate at the tempering condition:

$$W_{\text{vap}} = \frac{m_o q_s}{h_{vto}} + m_o \dot{m}_g$$

For the present example, W_{vap} is calculated to be 0.86 kg/s, which is significantly less than that for two-phase venting. With a set pressure of 0.345 bar·g, the vapor discharge is unchoked. It suffices to use the "isothermal" vapor/gas flow approximation, which in the subsonic region is given by:

$$\frac{G_{\text{vap}}}{\sqrt{P_o(\rho_{vo} + \rho_{go})}} = \frac{P_a}{P_o} \sqrt{-2 \ln \left(\frac{P_a}{P_o} \right)} \quad (35)$$

With a combined vapor/gas density of 0.88 kg/m³, Eq. 35 gives a vapor mass flux of 200 kg/m²·s. This yields a required vent area of 0.0044 m² for vapor venting. Note that this area is about the same as that for two-phase relief venting yielding $\Delta P/P_o$ of about 2.3 which also coincides with the design pressure of the vessel. Hence, for the present example, the required vent size for two-phase relief is essentially the same as that evaluated for vapor/gas venting only. It should be noted, however, that the chosen vent area should never be smaller than the vapor venting requirement.

Limiting Solutions

The present analytical treatment for venting of a hybrid reaction system can further provide limiting solutions at both ends: pure vapor system and pure gassy system. For the case of a pure vapor system with $y_{go} = 0$, Eq. 23 for τ simply yields the result given by Eq. 26a, which can be rewritten as:

$$\tau = 1 - \left[\frac{h_{vto} V_o W_v}{m_o^2 q v_{vto}} \right]^{0.5} \quad (26b)$$

where subscript v in W_o denotes the pure vapor system. This result is in perfect agreement with the τ expression obtained for a pure vapor system in an earlier paper (Leung, 1986). Substitution of Eq. 26a into the expression for temperature, Eq. 18, we obtain after some re-arrangement:

$$\frac{W_v}{W_{vo}} = \frac{1}{\left\{ 1 + \left[\frac{b}{T_o} (1 - \alpha_o) \omega_s \Delta T^* \right]^{1/2} \right\}^2} \quad (36a)$$

which upon substituting the definitions for W_{vo} , b , and ω_s yields:

$$W_v = \frac{m_o q}{\left[\left(\frac{V_o h_{vto}}{m_o v_{vto}} \right)^{1/2} + (C_p \Delta T)^{1/2} \right]^2} \quad (36b)$$

Again the above expression for relief vent rate is identical to that derived in connection with the vapor boiling system (Leung, 1986). Note that W_{vo} in Eq. 36a is the relief vent rate corresponding to zero overpressure in such a vapor system.

Now for the case of a pure gassy system with $y_{go} = 1$, Eq. 23 for τ reduces simply to the result given by Eq. 25. This turnaround time, unlike the pure vapor system, is independent of the vent rate. Since the term $(1 - \tau)$ represents the fractional mass remained at turnaround (see Eq. 16), this quantity is therefore independent of W or overpressure also. Substituting Eq. 25 for τ into Eq. 20 gives:

$$W_g = \frac{W_{go}}{P_g^*} \frac{1}{(1 + \sqrt{\alpha_o})^2} = \frac{m_o \dot{m}_g v_{go}}{(1 + \Delta P/P_o) v_o} \frac{1}{(1 + \sqrt{\alpha_o})^2} \quad (37)$$

while noting that P_g^* is $1 + \Delta P/P_o$ for the pure gassy system. The first term on the right side $W_{go}/(1 + \Delta P/P_o)$ in Eq. 37 is simply the required vent rate at the maximum pressure based on the entire vessel content m_o ; in other words, no mass loss during the overpressure period is assumed. By designating this vent rate as:

$$W_{gm} \equiv \frac{m_o \dot{m}_g v_{gm}}{v_o} = W_{go} \frac{P_o}{P_m} \quad (38)$$

we can rewrite Eq. 37 as:

$$\frac{W_g}{W_{gm}} = \frac{1}{(1 + \sqrt{\alpha_o})^2} \quad (39)$$

This result gives a simple relationship between the vent rate incorporating transient pressure buildup as well as mass loss and the vent rate based on a pointwise volumetric balance given by Eq. 38. Relative reduction in the vent rate is quite significant, about 40% at α_o of 0.1 and 75% at α_o approaching 1.0. Note also that W_{go} is simply the relief vent rate corresponding to zero overpressure for a gassy system.

It is important to recognize that the runaway behavior of a pure gassy system is independent of venting. The temperature heatup transient, as described by the energy equation, Eq. 3, is not tempered in any way due to the absence of latent heat of cooling. For such a system, it is prudent to consider the maximum gas generation rate, $\dot{m}_{g,\text{max}}$ when performing the vent sizing evaluation using Eqs. 37 and 38. Experimentally it can be estimated from the maximum pressure rise rate measured in an appropriate calorimeter via

$$\dot{m}_{g,\max} = \frac{V_c M_{wg}}{RT} \left(\frac{dP}{dt} \right)_{\max} / m_i \quad (40)$$

where V_c is the free-board volume occupied by the gas in the test apparatus, and m_i is the test sample mass. Thus, the only means of pressure relief of a gassy reaction is to remove the vessel content via venting. Attempt to take credit for early mass removal prior to attaining the maximum rate can be nonconservative and clearly a great deal more needs to be known in connection with the in-vessel hydrodynamic behavior of the particular reacting system.

Additional Comparison

To provide further validation of the analytical solution in vent sizing application, the above H_2O_2 example is purposely distorted to explore a wider range of system behavior, particularly in terms of the hybrid system parameter K . Two such distorted cases are examined here. In the first case, the reference gas generation rate \dot{m}_g as used in the H_2O_2 example was multiplied by a factor of 0.1. This reduced gas generation resulted in a higher tempering temperature at relief (from 106°C to 111.3°C) and an order of magnitude increase in K value (from 0.0135 to 0.16). The first case is hence closer in behavior to a vapor system. Figure 9 demonstrates good agreement between the analytical solutions and the exact solutions in terms of both W and A .

It is noted that at a normalized overpressure corresponding to $\Delta P/P_s = 1.0$, the required vent rate and vent area approach asymptotic values. As discussed elsewhere (Leung and Fisher, 1989), this is due to the Arrhenius behavior of the runaway reaction. Typically the higher the activation energy, the lower is the overpressure at which this asymptotic behavior is reached. This behavior tends to be more pronounced in vapor or near vapor systems. At similar overpressure, the corresponding "overtemperature" is usually much larger in vapor systems. For near gassy system, the overpressure is due mostly to gas accumulation and the quantity $\Delta P/\Delta T$ is typically much larger than that for a vapor pressure system, hence the overtemperature is comparatively smaller. Higher overtemperature in the

case of (near) vapor system implies that the specific reaction rate at pressure turnaround can be significantly higher than that at the initial relief condition. Hence, continued increase in overpressure (and also overtemperature) only leads to diminishing decrease in vent size; as this case shows, an asymptotic vent size is quickly approached at a $\Delta P/P_s$ value of about unity.

In the second case, the reference rate \dot{m}_g was increased by a factor of 10, yielding a system that is "gassier" in behavior. Here the hybrid system parameter is about 20 times smaller ($K=0.0007$) and the tempering temperature is 80°C. The analytical solutions in Figure 9 again demonstrate good agreement with the exact results. Since K is a key parameter in hybrid system characterization, the more than two orders of magnitude variation in this study clearly supports the validity of the analytical solution in vent sizing application.

Acknowledgment

Discussion on this topic with DIERS Users Group Members, particularly H. G. Fisher (Union Carbide Corp.) and H. S. Forrest (Lumus Crest Inc.), is much appreciated.

Notation

A	= ideal vent area
C_p	= liquid specific heat
G	= mass flux, mass flow rate per unit area
G^*	= normalized mass flux
G_{vap}	= vapor mass flux
h_{vf}	= latent heat of vaporization
K	= dimensionless group as defined by Eq. 24
m	= instantaneous mass in vessel
m_o	= initial mass in vessel
m_g	= mass of noncondensable gas
\dot{m}_g	= specific mass production rate of gas
M_{wv}	= molecular weight of vapor
M_{wg}	= molecular weight of gas
P	= system pressure
P_o	= ambient or back pressure
P_c	= choking pressure at the throat
q	= specific heat release rate
R	= gas law constant
t	= time
t_e	= emptying time, Eq. 13
T	= system temperature
V_o	= vessel internal volume
V_g	= volume occupied by gas
v	= specific volume
W	= relief vent rate or mass flow rate
W_{vap}	= vapor vent rate
W_{go}	= fundamental vent rate for gas generation, Eq. 15
W_{vo}	= fundamental vent rate for vapor generation, Eq. 14
x_v	= mass fraction of vapor
x_g	= mass fraction of gas
y_g	= mole fraction of gas in vapor phase

Greek letters

τ	= dimensionless turnaround time in pressure
ω	= critical flow scaling parameter, Eq. 8
α	= void fraction or volume fraction
ρ	= density
ΔT	= temperature rise above set
ΔP	= overpressure, pressure rise above set

Subscripts

adi	= adiabatic
g	= noncondensable gas phase
i	= inlet
ℓ	= liquid phase
m	= at maximum pressure

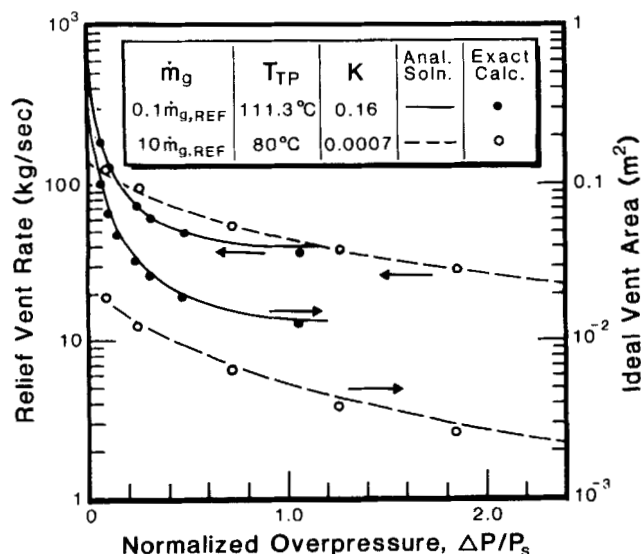


Figure 9. Additional comparison from parametric study.

max = maximum rate
o = initial, inlet stagnation
s = relief set point
t = throat
TP = tempering point
vap = pertaining to vapor venting
vl = difference between vapor phase and liquid phase

Superscript

- = average value during overpressure relief

Literature Cited

- Bird, R. B., W. E. Stewart, and E. N. Lightfoot, *Transport Phenomena*, Example 15.5-3, p. 480, Wiley, New York (1960).
Duxbury, H. A., "Relief System Sizing for Polymerization Reactors," *The Chem. Engr.*, p. 31 (Jan., 1980).
Fauske, H. K., "Generalized Vent Sizing Nomogram for Runaway Chemical Reactions," *Plant/Operations Prog.*, **3**(4), 213 (Oct., 1984).
Fisher, H. G., "DIERS Research Program on Emergency Relief Systems," *Chem. Eng. Prog.*, **81**(8), 33 (Aug., 1985).

- Huff, J. E., "Emergency Venting Requirements," *Plant/Operations Prog.*, **1**(4), 211 (Oct., 1982).
Huff, J. E., "Emergency Venting Requirements for Gassy Reactions from Closed-System Tests," *Plant/Operations Prog.*, **3**(1), 50 (Jan., 1984).
Leung, J. C., "Simplified Vent Sizing Equations for Emergency Relief Requirements in Reactors and Storage Vessels," *AIChE J.*, **32**(10), 1622 (1986).
Leung, J. C., H. K. Fauske, and H. G. Fisher, "Thermal Runaway Reactions in a Low Thermal Inertia Apparatus," *Thermochimica Acta*, **104**, 13 (1986).
Leung, J. C., "Overpressure During Emergency Relief Venting in Bubbly and Churn-Turbulent Flow," *AIChE J.*, **33**(6), 952 (1987).
Leung, J. C., and H. K. Fauske, "Runaway System Characterization and Vent Sizing Based on DIERS Methodology," *Plant/Operations Prog.*, **6**(2), 77 (1987).
Leung, J. C., and H. G. Fisher, "Two-Phase Flow Venting from Reactor Vessels," *J. Loss Prev. Process Ind.*, **2**(2), 78 (1989).
Leung, J. C., and M. Epstein, "Flashing Two-Phase Flow Including the Effects of Noncondensable Gases," *ASME Trans. J. of Heat Transf.*, **113**(1), 269 (1991).

Manuscript received Dec. 5, 1991, and revision received Mar. 19, 1992.